larger extracellular K accumulation has also been observed in the giant axon of the squid (*8*). This may be due in part to larger K currents (of the order of milliamperes per square centimeter as compared to a few microamperes in heart muscle).

Figure 2 shows the results obtained when clamp pulses of fixed duration, 3.4 seconds, were applied to study the afterpotential as a function of the clamped membrane potential in greater detail. The duration of a test action potential generated 800 msec after release of the clamp is compared to that of a normal action potential. The membrane current at the end of the clamp pulse, the afterpotential, and the action potential shortening are plotted against the clamped membrane potential. Both afterpotential and action potential shortening yield N-shaped relations similar to the current-voltage relation. Such results indicate that the K efflux has a minimum in the same voltage region as the membrane current.

In the experiment of Fig. 3, a K-sensitive microelectrode directly monitoring the local extracellular K activity was inserted into another preparation. The electrodes were prepared by filling the glass micropipette with a liquid ion exchange resin (*4*, *9*). The tip diameter was ~ 1 μm and the electrochemical response time ranged between 15 and 25 msec (*10*). With the electrode placed in the muscle, the measured potential is the sum of the potential caused by changes in the K activity and the electrical potential in the extracellular space. During the application of a voltage clamp step the flow of current through the series resistance adds to the electrical signal resulting from K accumulation. However, after the release of the clamp step, when there is no applied current, the K electrode trace mainly represents the K activity in the extracellular space and exhibits a slowly decaying tail similar to the time course of the afterpotential (Fig. 3A). In Fig. 3D the current at the end of the clamp, the afterpotential, the signal from the K-sensitive microelectrode, and the action potential shortening are all plotted against the clamped membrane potential. In this experiment the afterpotential and the response from the K electrode were measured just before the test action potential was generated in order to obtain a more accurate estimate of the extracellular K^+ concentration at the time of the test action potential generation. Note that the three parameters used to estimate the extracellular K concentration all yield N-shaped relations with a minimum around –20 mv, similar to the steady state current-voltage relation. These results provide strong evidence for inward-going (anomalous) rectification of the K current. Although the negative slope of the steady state current-voltage relation between –40 and –20 mv could be explained by the turn-on of an inward current component (Na or Ca), the decreasing accumulation in this region can only be explained by the turn-off of the K current.

Although afterpotential, K electrode, and action potential shortening give basically the same voltage dependence for the K accumulation, there are minor systematic differences. The action potential shortening after clamps to or above plateau level is often greater than that observed when the same afterpotentials are obtained after clamps to lower voltages. This effect is most prominent when the action potential is stimulated shortly after the end of the clamp. The action potential prolongation following hyperpolarizing clamps is often very small, although there is a considerable hyperpolarizing afterpotential. In Fig. 3A the K electrode potential has a smaller shift and a slower initial decay than the afterpotential. This suggests that the K electrode either is less sensitive to K than the myocardial membrane or is exposed to a smaller change in the K concentration. The first possibility is tested by the experiment in Fig. 3C, where the K concentration is changed from 3 to 6 m*M*. The very similar depolarizations measured with the K electrode (11 mv) and the intracellular microelectrode (12 mv) do not, however, indicate significant differences in K selectivity. The afterpotential probably reflects the average K concentration in the immediate vicinity of the membrane, while the K electrode measures a lower and more localized concentration change in one of the larger compartments of the extracellular space. The considerable outward current recorded at the minimum of the current-voltage relation in combination with little or no depolarizing afterpotential suggests that the steady state current includes other components than the K current (such as the Cl current, the transgap leakage current, and the current associated with an electrogenic Na-K pump).

These experiments show that extracellular K accumulation does occur in frog ventricular muscle during long clamp pulses. The time and voltage dependence of the accumulation indicates that it is closely related to the membrane current and thus can be used as an indicator for K efflux. In this capacity the accumulation verifies inward-going K rectification.

LARS CLEEMANN, MARTIN MORAD
Department of Physiology, University of Pennsylvania School of Medicine, Philadelphia 19174

References and Notes

1. J. F. Lamb and J. A. S. McGuigan, *J. Physiol. (Lond.)* **195**, 283 (1968).
2. A. J. Brady and J. W. Woodbury, *ibid.* **154**, 385 (1960).
3. S. Weidmann, *ibid.* **132**, 157 (1956).
4. J. Walker, *Anal. Chem.* **43**, 89A (1971).
5. M. Morad and R. K. Orkand, *J. Physiol. (Lond.)* **219**, 167 (1971).
6. M. J. Keenan and R. Niedergerke, *ibid.* **188**, 235 (1967).
7. S. G. Page and R. Neidergerke, *J. Cell Sci.* **11**, 179 (1972).
8. B. Frankenhaeuser and A. L. Hodgkin, *J. Physiol. (Lond.)* **131**, 341 (1956), W. J. Adelman, Jr., Y. Palti, J. P. Senft, *J. Membr. Biol.* **13**, 387 (1973).
9. Corning No. 477317.
10. R. P. Kline and M. Morad, in preparation.
11. We thank R. P. Kline for providing us with K electrodes. Supported by PHS grant 16152.

20 June 1975; revised 22 September 1975

Serengeti Migratory Wildebeest: Facilitation of Energy Flow by Grazing

Abstract. *Dense concentrations of migratory wildebeest leaving the Serengeti Plains in late May 1974 reduced green plant biomass by almost 400 grams per square meter, 85 percent of the initial standing crop. However, this grazing prevented senescence and stimulated net primary productivity of the grasslands. Thomson's gazelles leaving the plains a month later were significantly associated with areas previously grazed by wildebeest, and this association was still evident at the end of the dry season, 6 months later.*

The Serengeti-Mara ecosystem is defined by the movement of the region's large herds of migratory grazers (*1*), and consists of core areas in Tanzania's Serengeti National Park and Kenya's Maasai-Mara Game Reserve, together with adjacent areas. This region contains "the greatest and most spectacular concentration of game animals found anywhere in the world" (*2*). The most recent population estimates suggest a 1974 population size of more than 1 million wildebeest (*Connochaetes taurinus albojubatus* Thomas) (*3*), 600,000 Thomson's gazelle (*Gazella thomsonii*) (*4*), 200,000 zebra (*Equus burchelli*) (*5*), and 65,000 buffalo (*Syncerus caffer* Spearman) (*6*), as well as undefined numbers of more than 20 other species of grazing animals. There is, however, very little information on the dynamics of the grasslands supporting this huge herbivore biomass. The information reported here on productivity of the grasslands along the western border of the Serengeti Plains indicates that the migratory wildebeest convert a senescent grassland into a highly

productive community, and that this conversion is related to the dry season exploitation patterns of Thomson's gazelle.

During May 1974, a large concentration of wildebeest built up over a 2-week period in Moru Kopjes, along the western border of the Serengeti Plains. This concentration was variously estimated at 50 to 70 percent of the total migratory population (*7*). On May 22 the mass began to move northward, and on May 23 an exclosure was established in a *Themeda-Pennisetum* grassland on one of the major migratory routes to the hills west of the plains. Green plant biomass and grazing table height were measured inside and outside of the exclosure over the following 32 days, and green biomass concentration, a measure of forage density, was calculated from these two measurements (*8*). Over the 4-day period it took for the wildebeest to pass through the area, they had a seemingly devastating impact on the plant community (Table 1), reducing green biomass by 84.9 percent, height by 56 percent, and biomass concentration by 65.7 percent. Because of the spacing pattern in such grazing herds, it seems likely that these reductions were the result of actual grazing, rather than trampling (*9*). The reduction of biomass concentration is a consequence of feeding selection for green leaf by the wildebeest; green biomass is reduced more severely than height, with many of the culms remaining standing but stripped of leaves after the wildebeest move through. Trampled areas were much more severely affected and did not recover from the wildebeest passage. Single comparison tests in analyses of variance revealed (i) no significant differences inside and outside the exclosure before the wildebeest passage, (ii) highly significant differences afterward, and (iii) highly significant differences in outside samples before and after the migratory wildebeest went through the area.

Over the 28 days after wildebeest passage, the grazed areas sustained a net primary productivity of 2.6 g m^{-2} day^{-1}, while the area protected from grazing had a green biomass decline of 4.9 g m^{-2} day^{-1} and trampled areas were completely unchanged (Fig. 1). Height continued to increase in the enclosed area, as a result of continued elongation of dense flowering culms. In the previously grazed area, height decreased, and regrowth after grazing was a result of vigorous tillering. This produced a short but dense mat of green leaf forage, and by 3 weeks after wildebeest passage a grazing lawn with a high biomass concentration had been produced.

Wildebeest grazing was decidedly patterned in the area, with certain stands only lightly grazed while others were grazed at an intensity comparable to that of the

Table 1. Impact of a 4-day passage of migratory wildebeest through grasslands dominated by *Themeda* and *Pennisetum* on the western border of the Serengeti Plains. The F values are from single contrast tests built into analyses of variance after it was determined that there were significant interaction terms in all analyses; degrees of freedom are 1, 21 in all cases; N.S., not significant.

Time	Biomass (g/m^2)	Height (cm)	Biomass concentration ($mg/10\ cm^2$)
	Fenced vegetation, wildebeest excluded		
Before	501.9	64	7.9
After	449.2	63	7.1
	F = 0.217	F = 0.010	F = 0.123
	N.S.	N.S.	N.S.
	Vegetation subject to wildebeest grazing		
Before	457.2	66	6.9
After	69.0	29	2.4
	F = 137.561	F = 25.948	F = 15.279
	P = .005	P = .005	P = .05

Table 2. Relationship between occupance by Thomson's gazelle and vegetation properties on 25 June 1974, in the area previously subject to passage by the migratory wildebeest. Least significant difference (L.S.D.) is at P = .06.

Condition	Biomass (g/m^2)	Height (cm)	Biomass concentration ($mg/10\ cm^3$)
Gazelle present	80.7	15.4	5.48
Gazelle absent			
Low biomass	43.9	13.6	3.80
High biomass	160.5	63.6	2.56
	$F_{2\ 19}$ = 28.027	$F_{2\ 19}$ = 31.809	$F_{2\ 19}$ = 5.420
	P = .01	P = .01	P = .05
	L.S.D. = 4.0	L.S.D. = 2.0	L.S.D. = 1.53

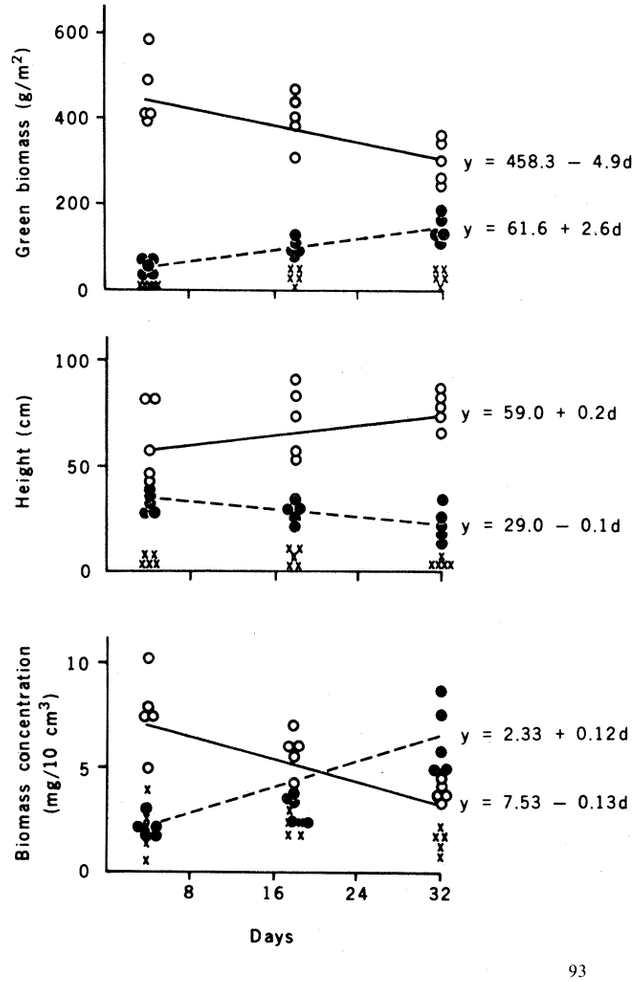

Fig. 1. Dynamics of vegetation properties after wildebeest passage through the western Serengeti Plains. Data are for (○) enclosed areas protected from wildebeest grazing, (●) unenclosed areas grazed by wildebeest, and (x) unenclosed areas showing evidence of trampling immediately after wildebeest passage. Lines are best-fit determined by the least-squares method where t indicated a significant time trend at $P \leq .05$. Best-fit equations are given at the end of each such line; d is time in days after wildebeest entered the area and y is the variable on the ordinate.

study stand. By 32 days after wildebeest reached the study site, substantial numbers of Thomson's gazelle were entering the area, and a transect was made of randomly located sites. Vegetation properties were measured, and the sites were scored according to the presence or absence of Thomson's gazelle. Sites where gazelle were absent could be stratified into low and high biomass stands, and the data indicated that gazelle entered the area of the vigorous regrowth and high forage density that followed wildebeest grazing (Table 2). The stands favored by gazelle had intermediate biomass, a short canopy, and high biomass concentration. Over the following 30 days, consumption by gazelle averaged 1.05 g m^{-2} day^{-1} in areas previously grazed by wildebeest, but only 0.27 g m^{-2} day^{-1} in areas not grazed by wildebeest (t = 6.916 for $P < .001$; d.f. = 9). In fact, consumption in areas not previously grazed by wildebeest could not be discriminated from zero (t = 1.825 for P not significant; d.f. = 9). The distinctive character of wildebeest-grazed stands, and the association of gazelle with them, was maintained throughout the dry season of 1974. A final transect through the area was done on 14 November 1974, just at the end of the dry season. Randomly chosen stands were scored as follows: wildebeest-grazed, gazelle present, 11; wildebeest-grazed, gazelle absent, 4; not grazed by wildebeest, gazelle present, 0; not grazed by wildebeest, gazelle absent, 8. This represents a significant (Fisher's exact P = .001) association between grazing by wildebeest during their migratory passage and dry season exploitation by gazelle.

Wildebeest and Thomson's gazelle are the two most abundant grazers in the Serengeti-Mara ecosystem. The mechanisms of coexistence of such numbers of large grazers in a small area have been studied for some time (*10*). The present data indicate that heavy grazing by the migratory wildebeest population as it leaves the Serengeti Plains prepares the plant community for subsequent dry season exploitation by gazelle. The association of gazelle with areas previously grazed by wildebeest suggests that coexistence of these two species is a consequence of coevolution that has partitioned the grassland exploitation patterns during the critical dry season. Rather than competition, there is facilitation of energy flow into the gazelle population by the wildebeest population through the impact of the latter on the plant community. In addition to converting a senescent plant community into a productive one, it seems likely that wildebeest grazing substantially improves forage quality. Nutrient content and digestibility are considerably greater in rapidly growing grasses than in mature tissues (*11*). It therefore seems likely that total nutrient and energy flow to the gazelle population is facilitated even more than is suggested by these data on net primary productivity and gazelle grazing.

S. J. McNAUGHTON

Biological Research Laboratories, Syracuse University, Syracuse, New York 13210, and *Serengeti Research Institute, P.O. Seronera, Via Arusha, Tanzania*

References and Notes

1. L. M. Talbot and M. H. Talbot, *Wildl. Monogr. 12* (1963).
2. J. G. Williams, *A Field Guide to the National Parks of East Africa* (Collins, London, 1967), p. 120.
3. This estimate was derived by fitting a line by the least-squares method (r^2 = 0.989) to the census data of A. R. E. Sinclair [*E. Afr. Wildl. J.* **11**, 93 (1973)] and M. Norton-Griffiths [*ibid.*, p. 135], covering the period from 1961 to 1972, and extrapolating the line to 1974.
4. R. Bradley, *Annu. Rep. Serengeti Res. Inst.* (1972), p. 32.
5. R. O. Skoog, *ibid.* (1970), p. 28.
6. J. J. R. Grimsdell, personal communication regarding 1974 total census.
7. R. H. V. Bell, D. A. Kreulen, T. Mcharo, personal communications after aerial observations of the concentration.
8. Green plant biomass was measured by the reflectrometric technique of C. J. Tucker, L. D. Miller, and R. L. Pearson [in *Proceedings, 2nd Annual Remote Sensing of Earth Resources Conference, 1973*, F. Shahroki, Ed. (Univ. of Tennessee Press, Tullahoma, 1973), pp. 601–627] after calibration on Serengeti grasslands. The calibration equation (r^2 = 0.955 for $P < .001$; d.f. = 18) is green biomass (in grams per square meter) = 109.8 R − 83.8, where R is the ratio of reflectances at 8000 and 6750 Å. Grazing table height was measured by allowing a Styrofoam sheet 17 by 26 cm, weighing 4.5 g, to come to rest in the canopy; the resting height represents a level where grazers would encounter physical resistance (D. F. Vesey-Fitzgerald, personal communication). Biomass concentration, expressed as milligrams of green biomass per cubic centimeter, is calculated for a cylinder whose height is the grazing table height and whose area and biomass are as specified in the reflectometric measurement. It was first determined that this value varies independently with both green biomass and height. It is assumed that biomass concentration is an index of the potential food yield per mouthful for a grazer, since the higher the biomass concentration, the denser the green forage in the grazing volume.
9. A. R. E. Sinclair, thesis, Oxford University (1970).
10. D. F. Vesey-Fitzgerald, *J. Mammal.* **41**, 161 (1960); H. F. Lamprey, *E. Afr. Wildl. J.* **1**, 63 (1963); M. D. Gwynne and R. H. V. Bell, *Nature (Lond.)* **220**, 390 (1968); L. D. Harris, *Colo. State Univ. Range Sci. Ser. No. 11* (1972).
11. D. C. H. Plowes, *Rhod. Agric. J.* **54**, 33 (1957); R. M. Bredon and J. Wilson, *E. Afr. Agric. For. J.* **29**, 134 (1963); B. Marshall, *ibid.* **32**, 375 (1967).
12. I thank the trustees and director of Tanzania National Parks for permission to reside and work in the Serengeti National Park; T. Mcharo, director of the Serengeti Research Institute (SRI), for inviting me to work there; and F. Banyikwa, F. Kurji (both of the SRI), and M. McNaughton for valuable assistance in collecting data. Supported by the NSF ecosystem studies program grant BMS74-02043 to Syracuse University, and by a grant of sabbatical leave from Syracuse University. This is SRI publication No. 207.

28 February 1975; revised 23 May 1975

Human Heart and Platelet Actins Are Products of Different Genes

Abstract. *The amino acid sequences of selected cyanogen bromide peptides from human blood platelet actin and human cardiac muscle actin were compared; it was found that, at position 129, platelet actin has threonine, and that cardiac muscle actin has valine. Thus human cytoplasmic and myofibrillar actins must be synthesized under the control of different genes.*

Actin has been identified in many kinds of cells including muscle, where it is the major constituent of the thin filament. Actin participates in several reversible intermolecular interactions, and one of these, the formation of "arrowhead" complexes (*1*) with a truncated form of myosin, heavy meromyosin, has been used to identify "actin" in both animal (*2*) and plant (*3*) cells. Actins have been isolated from various muscles as well as from nonmuscle sources, and comparisons of their properties reveals that the different actins are very similar with respect to molecular weight and amino acid composition, including the presence of one residue of the unusual amino acid N^{τ}-methylhistidine. The results suggest that the structure of actin has been conserved and recent studies have shown that, although not completely invariant, muscle actins from such diverse sources as rabbits (*4*) and fish (*5*) are extremely similar in amino acid sequence.

The presence of actin in different tissues within the same organism raises the question of whether these actins are the products of the same gene, and thus identical in sequence, or whether a given organism has multiple separate, independently controlled genes for actin. Previous studies that bear on this question have employed peptide pattern techniques, and have yield-

Human Platelet:	Phe-Glu-Thr-Phe-Asn-Thr-Pro-Ala-Hse
Human Cardiac Muscle:	Phe-Glu-Thr-Phe-Asn-Val-Pro-Ala-Hse
Rabbit Skeletal Muscle:	Phe-Glu-Thr-Phe-Asn-Val-Pro-Ala-Hse

Fig. 1. Comparison of the sequences of peptide CB-4 from three actins. These peptides correspond to residues 124-132 in rabbit skeletal muscle, and the Val → Thr substitution is at position 129.